https://doi.org/10.48048/tis.2025.9173

# Limonoid Extracted from *Chisocheton macrophyllus* Seeds and Their Cytotoxic Activity against MCF-7 Breast Cancer Cell Lines

**Dewa Gede Katja[1], Intan Rahmayanti[2], Nurlelasari[2], Siska Elisahbet Sinaga[3], Kansy Haikal[3], Al Arofatus Naini[4], Khalijah Awang[5] and Unang Supratman[2,3,*]**

*[1]Department of Chemistry, Faculty of Mathematics and Natural Sciences, Universitas Sam Ratulangi, Kampus Bahu, North Sulawesi 95115, Indonesia*
*[2]Department of Chemistry, Faculty of Mathematics and Natural Sciences, Universitas Padjadjaran, Sumedang 45363, Indonesia*
*[3]Central Laboratory of Universitas Padjadjaran, Sumedang 45363, Indonesia*
*[4]Research Center for Pharmaceutical Ingredients and Traditional Medicine, National Research and Innovation Agency (BRIN), Cibinong Science Center Complex, West Java 16911, Indonesia*
*[5]Department of Chemistry, Faculty of Science, University of Malaya, Kuala Lumpur 59100, Malaysia*

**([*]Corresponding author's e-mail: unang.supratman@unpad.ac.id)**

*Received: 18 October 2024, Revised: 26 October 2024, Accepted: 2 November 2024, Published: 10 January 2025*

**Abstract**

Meliaceae family consists of various plants that have been used as a source of medicinal plants and limonoid compounds. Limonoid is a compound group of terpenoid which has many bioactivities. One of the species from Meliaceae which produced limonoids is *Chisocheton macrophyllus*. The *n*-hexane fraction of the *C. macrophyllus* seed afforded 3 limonoids, namely 7-deacetylepoxyazadiradione (**1**), 6α-acetoxydeoxygedunin (**2**) and 6α-acetoxygedunin (**3**). Data from a variety of spectroscopic techniques, including as mass spectroscopy, FTIR, 1- and 2-dimensional NMR, were used to identify the secondary metabolite structures, and the PrestoBlue™, method was used for the cytotoxic assay. Compound (**2**), known as 6α-acetoxydeoxygedunin, was first reported in this genus. MCF-7 breast cancer cell lines have also been used to assess limonoids compounds (**1** - **3**). The **2** and **3** were categorized as weak with an $IC_{50}$ value of 231.26 and 475.87 µg/mL, while compound **1** showed inactive with $IC_{50}$ values of > 500 µg/mL. These findings encourage further exploration of Meliaceae plants for new bioactive compounds and advance the development of novel cancer treatments.

**Keywords:** Cytotoxic activity, *Chisocheton macrophyllus*, MCF-7 cell lines, Limonoids

## Introduction

The Meliaceae family has been thoroughly investigated for drug discovery, and it is an established source of potentially therapeutic chemicals [1]. Terpenoid compounds from this family are generated by several genera, such as *Dysoxylum*, *Aglaia*, *Chisocheton* and *Lansium*. From among the numerous structures, these terpenoids exhibit bioactivities such as anti-inflammatory, anti-cancer and anti-malarial properties [2-5]. One of the secondary metabolites included in the terpenoid group is limonoid. This compound loses terminal carbons as much as 4 to form a tetracyclic structure with A, B, C and D rings in its apotirucallane skeleton, and is the source of the 26 carbon (C26) skeleton seen in limonoids. The D ring often undergoes oxygenation to form either furan or lactone rings [6-8]. Owing to significant oxidation and rearrangement activities, limonoids isolated from Meliaceae species exhibit various structures [9]. This structural diversity contributes to several kinds of biological functions, including antifeedant, antifungal, antibacterial, antimalarial, antiviral and cytotoxic effects [10-12]. One of the Meliaceae genera which is famous for its medicinal properties and is widespread in Asia,

especially in Indonesia and Malaysia is *Chisocheton* [13].

Several researchers have reported that many limonoid compounds have been isolated from *Chisocheton* species and show significant effect against breast cancer cells, such as pentandricines A - D from *Chisocheton pentandrus* [14,15], ceramicin A - D from *C. ceramicus* and disobinin, azadiradione, mahonin, epoxyazadiradione and 6α-acetoxiepoxyazadiradione from *C. siamensis* [16-18]. Furthermore, the potential of this genus in producing limonoid compounds was demonstrated by chisonimbolinin A - G from *C. paniculatus* and 14-deoxyxyloccensin K from *C. ceramicus* [19,20]. Nurlelasari *et al.* [20] succeeded in isolating a new havanensin class limonoid from *C. macrophyllus* seeds [21]. Based on previous research, several limonoids have been isolated from *n*-hexane and have diverse activities. So, we wanted to know more about the limonoid content of *n*-hexane extract from *C. macrophyllus* seed. This provides a great opportunity to identify new limonoid structures and assess their activity through various compound isolation methods and activity assays. Limonoid chemicals can impede the formation of cancer cells, which cause cell death [22,23]. Cancer continues to be a major health issue globally and in Indonesia, particularly breast cancer. The 11.6 % of new cases of cancer globally in 2022 were breast cancer cases, with a high death rate [24]. This underscores the urgent need for effective anticancer agents. Natural compounds, such as limonoids, represent a promising avenue for drug discovery due to their structural diversity and pharmacological versatility. Given the promising pharmacological profile of limonoids, *C. macrophyllus* seeds were selected for further investigation. The present study focused on the cytotoxic effects of 2 forms of the limonoid gedunin and havanensin isolated from *C. macrophyllus* seeds. These compounds were evaluated for their cytotoxic activity against MCF-7 cells, a widely used human breast cancer cell line. MCF-7 cells were selected for testing because they represent estrogen receptor-positive (ER+) breast cancer, which is one of the most common subtypes of breast cancer. This cell line is a well-established model for screening potential anticancer agents due to its relevance in clinical research and the availability of comparative data.

## Experimental section

### General experimental procedures

A Perkin Elmer Spectrum 100 FT-IR spectrometer (Shelton, Connecticut, USA) equipped with a NaCl plate was used to interpret the infrared spectra. The spectra of mass fragmentation were ascertained with a Waters Quadrupole Time-of-flight Mass Spectrometer (Waters, Milford, Massachusetts, USA). Every compound's NMR spectra were recorded using a JEOL JNM-ECX500R/S1 spectrometer (Tokyo, Japan) operating at 500 MHz for $^{1}H$ and 125 MHz for $^{13}C$, using TMS as the internal standard. Compound separation was performed using vacuum liquid chromatography with silica gel $G_{60}$, and column chromatography with silica gel (70 - 230 and 230 - 400 mesh, Merck, Darmstadt, Germany) guided by thin-layer chromatography (TLC) with silica $GF_{254}$ plates (Merck, 0.25 mm), ODS plates and detection reagents such as 10 % sulfuric acid (*v/v*) in ethanol and Ehrlich's reagent (1 g *p*-dimethylaminobenzaldehyde (DMAB) and 10% sulfuric acid in ethanol). For cytotoxic activity testing, PrestoBlue™ reagent, Breast cancer cells MCF-7, cultured in RPMI 1640, fetal bovine serum (FBS) as much as 10%, trypsin-EDTA, dimethyl sulfoxide (DMSO), and cisplatin as a positive control were used

### Plant material

The sample was *C. macrophyllus* seeds which were gained from Botanical Garden, Bogor, West Java Province, Indonesia. The sample was determined with number of specimen (No. Bo-1295453) at Biology Research Laboratory, Universitas Padjadjaran, Jatinangor, Indonesia.

### Isolation of compounds from the seeds of *Chisocheton macrophyllus*

Methanol was used to extract dried *C. macrophyllus* seed powder (4.5 kg). The extract methanol had been evaporated to gain 560 g yield. After that, the fractionation with the following solvents, *n*-hexane, ethyl acetate and *n*-butanol were done at room temperature. The result of fractionation was concentrated and collected to get 346.64 g of *n*-hexane fraction, 60.8 g of ethyl acetate fraction and 14.6 g of *n*-butanol fraction. The preliminary testing to check the presence of limonoids was done using thin-layer chromatography (TLC) with Ehrlich's reagent as the

detection agent. The appearance of a red color on the TLC plate after spraying with Ehrlich's reagent indicated the presence of limonoids in the n-hexane fraction.

The concentrated fraction of *n*-hexane was divided using VLC (silica gel G60) as the fixed stage and the combination of *n*-hexane (nonpolar), ethyl acetate (semi polar) and methanol (polar) was used as much as 10% gradient as the mobile phase, resulting in 13 fractions (A - M). Fraction F (in the range of to 4.4 g) was divided using gradient solvent (5%) with column chromatography, yielding 12 parts (F1 - F12). Using column chromatography with *n*-hexane, methylene chloride and ethyl acetate (2:7.5:0.5 isocratic), as much as 1.2 g of F5 was further dissociated to afford 4 subparts (F5A - F5D). Subpart F5D as much as 308.3 mg had been parted with isocratic solvent, (1) *n*-hexane: (8.5) methylene chloride: (0.5) ethyl acetate, resulting in compound 1 (12.8 mg). Column chromatography was used to segregate fraction I (4.5 g) with a gradient of *n*-hexane and ethyl acetate (5%), yielding 5 subfractions (I1 - I5). The *n*-hexane, chloroform and ethyl acetate (4:5.5:0.5 isocratic) were used for separating the subfraction I3 (1.3 g) with column chromatography, resulting in compound 2 (3.0 mg). The 5% gradient of *n*-hexane: ethyl acetate solvents was used in dividing fraction J (1.5 g), yielding J1 - J19. Compound **3** was found from subpart J9 (50.3 mg) using column chromatography with *n*-hexane, methylene chloride and ethyl acetate (4:5.5:0.5) isocratic.

**Spectroscopic data**

Compound **1**: White powder; $[\alpha]^{27}_{D}$ + 28.2 ° (c 0.2, methanol); UV (Methanol) $\lambda_{max}$ 220 nm; Infrared (KBr) $\nu_{max}$ 3,517, 2,928, 1,741, 1,669, 1,500, 1,367, 1,385 and 1,253 $cm^{-1}$; HR-TOFMS, *m/z* 425.2321 $[M + H]^+$, (calculated for $C_{26}H_{33}O_5$, *m/*z 425.2328); $^1$H-NMR ($CDCl_3$, 500 MHz); 7.16 (1H, d, 10.5), 5.84 (1H, d, 10.5), 2.40 (1H, dd, 2.5, 13.0), 1.63 (2H, m), 3.63 (1H, d, 2.6), 2.63 (1H, dd, 4.0, 12.5), 1.96 (2H, m), 1.80 (1H, m), 2.13 (1H, m), 3.53 (1H, s), 3.88 (1H, s), 1.03 (3H, s), 1.17 (3H, s), 7.51 (1H, s), 6.21 (1H, d, 1.45), 7.38 (1H, d,1.5), 1.10 (3H, s), 1.07 (3H, s), 1.12 (3H, s) and $^{13}$C-NMR ($CDCl_3$, 125 MHz); 158.3 (C-1), 125.7 (C-2), 204.9 (C-3), 44.4 (C-4), 45.3 (C-5), 27.9 (C-6), 71.3 (C-7), 44.5 (C-8), 38.3 (C-9), 39.9 (C-10), 16.2 (C-11), 29.7 (C-12), 42.6 (C-13), 73.3 (C-14), 57.6 (C-15), 209.5 (C-16), 51.3 (C-17), 25.2 (C-18), 20.1 (C-19), 116.9 (C-20), 141.6 (C-21), 111.1 (C-22), 142.4 (C-23). 19.7 (C-24), 21.3 (C-25) and 27.2 (C-26).

Compound **2**: White powder; UV (methanol) $\lambda_{max}$ 215 nm; Infrared (KBr) $\nu_{ma}$x 2,922, 1,741, 1,668, 1,503, 1,365 and 1,244 $cm^{-1}$; HR-TOFMS *m/z* 525.2484 $[M + H]^+$, (calculated for $C_{30}H_{37}O_8$, *m/z* 525.2488); $^1$H-NMR ($CDCl_3$, 500 MHz); 7.08 (1H, d, 10.5), 5.85 (1H, d, 10.5), 2.70 (1H, d, 14.0), 5.30 (1H, dd, 12.0, 3.5), 4.54 (1H, d, 4.0), 2.47 (1H, dd, 19.0, 13.0), 1.61 (2H, m), 1.98 (2H, m), 5.70 (1H, s), 5.60 (1H, s), 1.21 (3H, s), 0.86 (3H, s), 7.40 (1H, s), 6.32 (1H, d, 1.45), 7.39 (1H, d, 1.5), 1.05 (3H, s), 1.14 (3H, s), 1.15 (3H, s), 2.33 (3H, s), 2.09 (3H, s) and $^{13}$C-NMR ($CDCl_3$, 125 MHz); 157.0 (C-1), 126.0 (C-2), 204.1 (C-3), 44.1 (C-4),46.1 (C-5), 69.8 (C-6), 73.3 (C-7), 42.6 (C-8), 40.1 (C-9), 39.5 (C-10), 18.4 (C-11), 26.0 (C-12), 38.8 (C-13), 158.2 (C-14), 111.0 (C-15), 167.5 (C-16), 78.3 (C-17), 24.7 (C-18), 18.4 (C-19), 120.4 (C-20), 141.2 (C-21), 109.9 (C-22), 143.1 (C-23), 27.2 (C-24), 19.8 (C-25), 22.7 (C-26), 21.2 (C-27), 177.7 (C-28), 21.1 (C-29) and 170.0 (C-30).

Compound **3**: White powder; UV (Methanol) $\lambda_{max}$ 215 nm; Infrared (KBr) $\nu_{max}$ 2,919, 1,740, 1,667, 1,502, 1,382 and 1,234 $cm^{-1}$; HR-TOFMS *m/z* 541.2440 $[M + H]^+$, (calculated for $C_{30}H_{37}O_9$, *m/z* 541.2438); $^1$H-NMR ($CDCl_3$,500 MHz); 7.06 (1H, d, 10.5), 5.95 (1H, d, 10.5), 2.52 (1H, d,13.0), 5.27 (1H, dd, 13, 2.5), 4.89 (1H, d, 2.5), 2.55 (1H, d, 12.5), 2.34 (2H, t, 7.5), 2.54 (1H, d, 5.5), 2.51 (1H, d, 5.5), 3.61 (1H, s), 5.61 (1H, s), 1.27 (3H, s), 1.20 (3H, s), 7.41 (1H, s), 6.32 (1H, d, 1.5), 7.43 (1H, d, 1.5), 1.25 (3H, s), 1.15 (3H, s), 1.32 (3H, s), 2.02 (3H, s), 2.14 (3H, s) and $^{13}$C-NMR ($CDCl_3$,125 MHz); 156.2 (C-1), 126.7 (C-2), 204.7 (C-3), 44.9 (C-4), 47.8 (C-5), 69.6 (C-6), 72.6 (C-7), 43.0 (C-8), 38.4 (C-9), 40.6 (C-10), 15.0 (C-11), 25.9 (C-12), 38.7 (C-13), 69.5 (C-14), 56.3 (C-15), 167.2 (C-16), 51.2 (C-17), 28.7 (C-18), 31.6 (C-19), 120.3 (C-20), 141.3 (C-21), 109.9 (C-22), 143.2 (C-23), 31.7 (C-24), 20.2 (C-25), 22.0 (C-26), 21.2 (C-27), 170.1 (C-28), 21.4 (C-29) and 170.3 (C-30).

**Determination of cytotoxicity**

The bioactivity evaluation was done following the method stated by Sinaga *et al.* [24]. The cytotoxic activity was determined using the PrestoBlue™ assay. MCF-7 cells were seeded into a microplate at a density

of $3\times10^4$ cells/cm³. Afterward, 1 mL of trypsin-EDTA solution was added, and the cells were incubated for 5 min. The incubated cells were transferred into a tube containing media and centrifuged at 3,000 rpm for 5 min, separating the supernatant and pellet. The supernatant was discarded, and the pellet was resuspended in media. The viability and number of cells were then assessed. The cells were cultured in a 96-well plate and incubated at 37 °C with 5% $CO_2$ for 24 h. After incubation, 100 µL of samples and cisplatin (positive control) were transferred from microtubes into each well. The plate was incubated again for another 24 h, and the media was removed from each well. A mixture of PrestoBlue™ reagent and media (10 µL reagent in 90 µL media) was added to each well and incubated for 1 - 2 h until a color change occurred. Absorbance was measured at 570 nm (reference: 600 nm) using a multimode reader. The $IC_{50}$ values were calculated to evaluate the cytotoxic activity of the isolated limonoid compounds.

## Results and discussion

### The results of compound isolation

Limonoids **1 - 3** were found on *n*-hexane fraction of *C. macrophyllus* seeds with purification process with several column chromatography methods, repeatedly. Compound **1** found in white powder form, soluble in acetone and chloroform. Thin-layer chromatography analysis produced a red color after spraying with Ehrlich's reagent. Additionally, this compound fluoresced under UV light at 254 nm but did not fluoresce under UV light at 365 nm. Based on UV spectrum analysis (**Figure 1**), Compound **1** showed absorption at a wavelength within 220 nm. The presence of a $\pi \rightarrow \pi^*$ electronic transition originating from an *α,β*-unsaturated ketone chromophore was proven by the absorption at 220 nm [26]. Therefore, Compound **1** was inferred to have an *α,β*-unsaturated ketone chromophore.

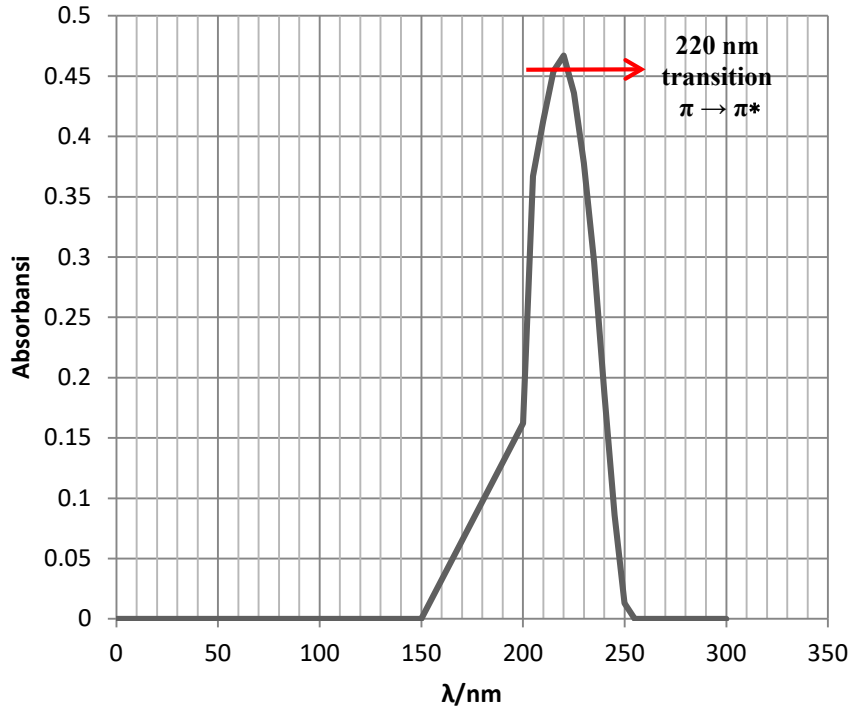


**Figure 1** The UV spectrum of compound **1**.

This inference was further supported by infrared spectrophotometer data (**Figure 2**), which displayed absorption at 1,669 $cm^{-1}$, characteristic of carbonyl stretching vibrations in unsaturated compounds. Other data were appeared on 3,517 $cm^{-1}$ (hydroxyl group), 2,928 $cm^{-1}$ (carbon-hydrogen $sp^3$), 1,741 $cm^{-1}$ (carbonyl group), 1,500$cm^{-1}$ (carbon double bond), 1,367, 1,385 $cm^{-1}$ (*gem*-dimethyl) and 1,253 $cm^{-1}$ (carbon-oxygen

stretching). This compound was confirmed by HRTOF-MS mass spectrum (**Figure 3**), showing a molecular ion signal with *m/z* 425.2321 $[M + H]^+$. The calculation of molecular mass for $C_{26}H_{33}O_5$ is *m/z* 425.2328 with the unsaturation degree is 11.

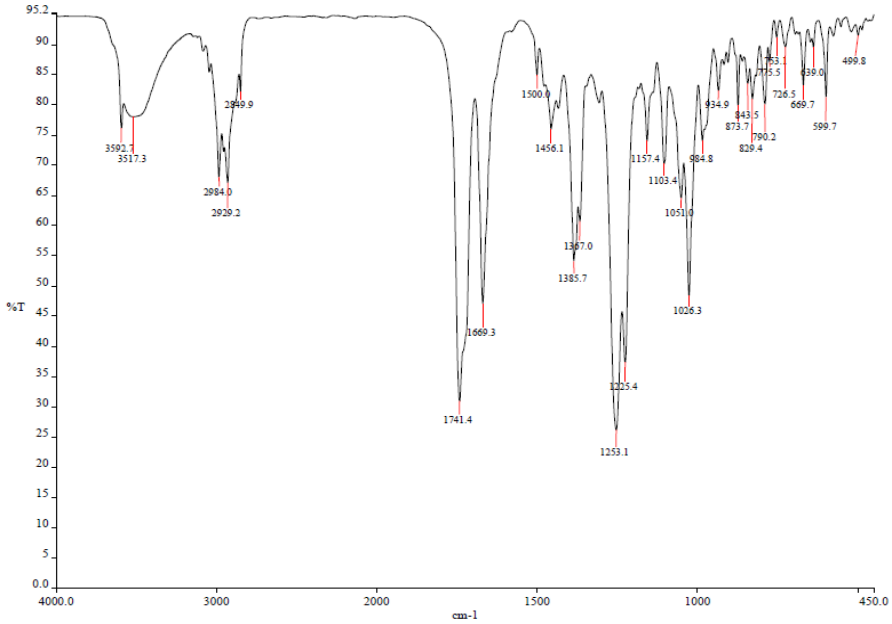


**Figure 2** FT-IR spectrum of (**1**).

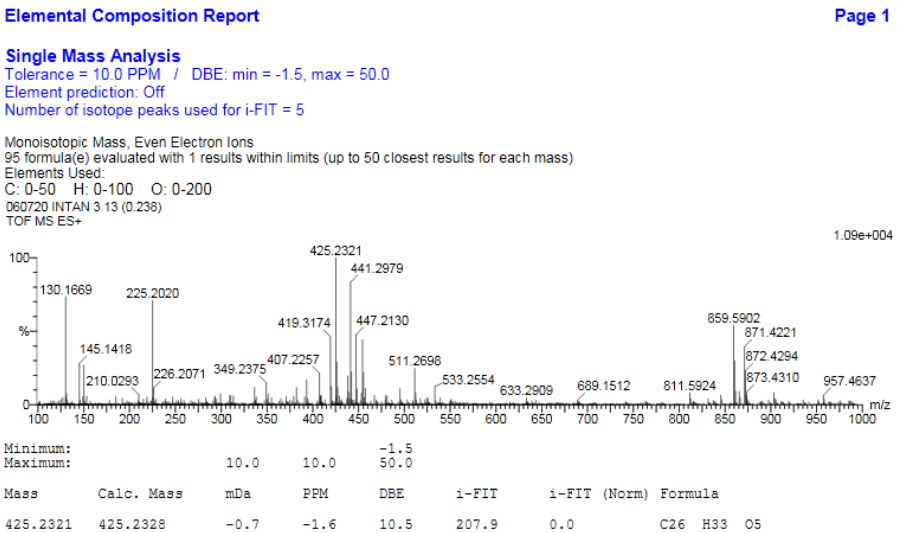


**Figure 3** HRTOF-MS spectrum of (**1**).

The divination was asserted by NMR spectra. The proton NMR spectrum (**Figure 4**) denoted the existence of 5 singlet signals for tertiary-methyl protons at $\delta_H$ 1.03, 1.07, 1.10, 1.12 and 1.17 ppm (3H). Signals for $sp^3$ protons appeared at hydrogen chemical shift 1.63, 1.80, 1.96, 2.13, 2.40, 2.63 and 3.88. Two oxygenated-proton $sp^3$ resonated at $\delta_H$ 3.53 and 3.63 ppm. Furan characteristic signals appeared at $\delta_H$ 7.51, 6.21 and 7.38 ppm, along with 2 olefinic-protons at $\delta_H$ 5.84 and 7.16. The $^{13}$CNMR and DEPT-135 spectra of compound **1** (**Figure 5**) exhibited 26 carbon signals. These included 5 methyl groups, 3 methylene, 3 methine $sp^3$, 3 methine groups $sp^2$, 2 $sp^3$ oxygenated methine groups and 2 oxygenated $sp^2$ methine groups. Furthermore, there

were 4 $sp^3$ quaternary, 1 $sp^3$ oxygenated quaternary carbon, 1 $sp^2$ quaternary carbon and 2 C=O.

Posit the interpretation of the $^1$H-NMR spectroscopy, compound **1** was suspected to have a limonoid skeleton, evidenced by the characteristic chemical shifts for a furan ring, which was believed to be a side chain of the limonoid structure. Compound **1** was predicted and consisted of 26 carbons, 32 protons and 5 oxygens. This was encouraged by the interpretation of the carbon and $^1$H-NMR data, which included 1 furan ring, 2 carbonyl groups, 1 oxygen likely from an epoxide group and another oxygen possibly from a hydroxyl group as a substituent on the structure of compound **1**. This was approved by the infrared spectrum data, with an absorption at 1,253cm$^{-1}$ showed the present of carbon-oxygen ether stretching and an absorption at 3,517 cm$^{-1}$ for OH-stretching.

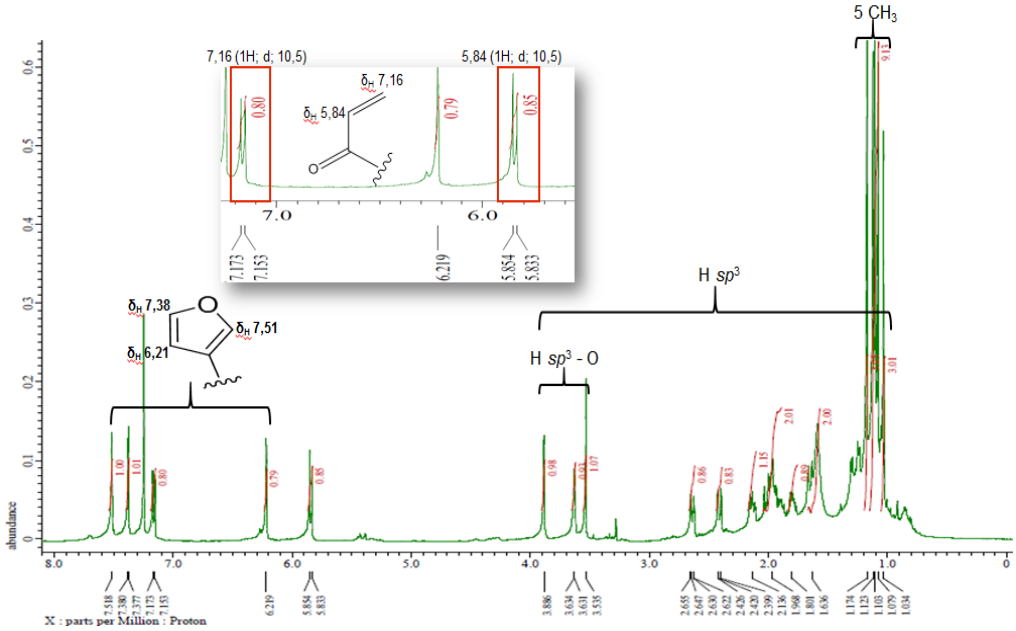


**Figure 4** $^1$H-NMR spectra of (**1**) (500 MHz in $CDCl_3$).

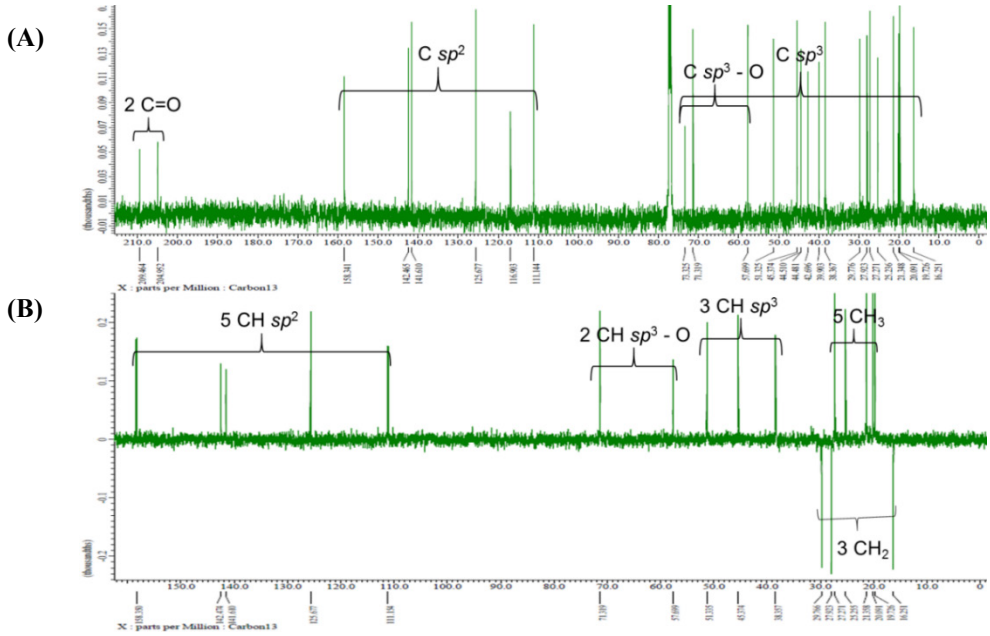


**Figure 5** $^{13}$C-NMR (A) and DEPT 135 (B) spectra of (**1**) (125 MHz in $CDCl_3$).

The proton, carbon and DEPT spectra were corroborated with HMQC-spectral data (**Figure 6**). The HMQC spectra indicated correlations between H-18/C-18, H-29/C-29, H-28/C-28, H-30/C-30 and H-19/C-19, confirming the apparency of 5 tertiary $CH_3$ groups in the structure of compound **1** ($\delta_C$ 25.2, 21.3, 19.7, 27.2 and 20.1 ppm). Additionally, correlations between H-6/C-6, H-11/ C-11 and H-12/ C-12 ($\delta_C$ 27.9, 16.2 and 29.7 ppm) verified the presence of 3 methylene groups in the structure of compound **1**. There were correlations between H-15/C-15 and H-7/C-7, confirming the presence of 2 oxygenated $sp^3$ methines in the structure of compound **1**. This suggested OH to C-7 and an epoxide C-14/C-15. Correlations between H-2/C-2 and between H-1/C-1 indicated the presence of an olefinic bond between C-1/C-2. Additionally, correlations between H-22/C-22, H-21/C-21 and H-23/C-23 confirmed the presence of a furan ring substituent in the structure of compound **1**.

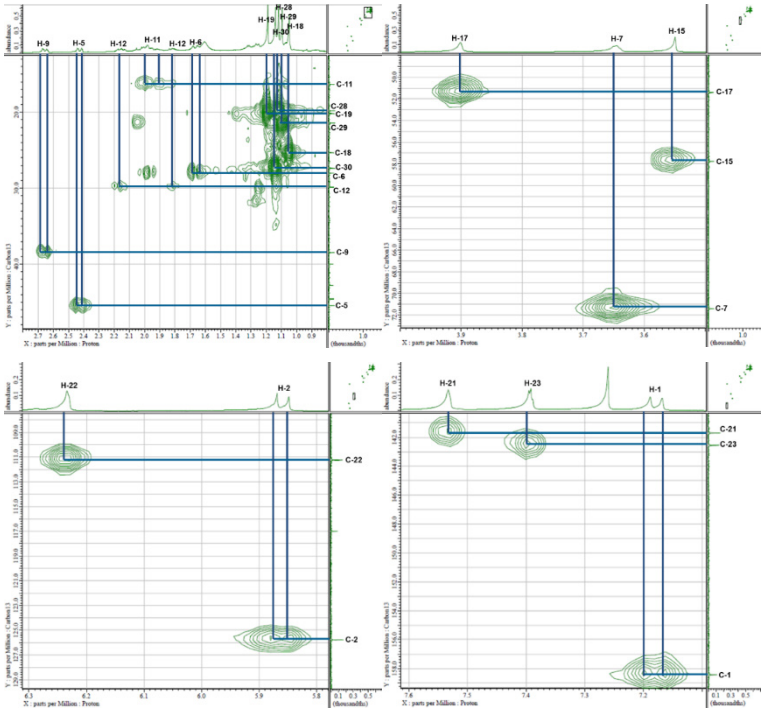


**Figure 6** Spectrum HMQC of **(1)**.

The information of $^1H$-$^1H$ COSY spectrum (**Figure 7**) presented correlations between protons attached to neighboring carbons. There were correlations between H-1 and H-2 ($\delta_H$ 7.16 with 5.84 ppm) and H-22 and H-23 ($\delta_H$ 6.21 with 7.38 ppm). Apart from that, there was a correlation between H6, H5 and H7 ($\delta_H$ 1.63 with 2.40 and 3.63 ppm), as well as a correlation between H9 and H11 ($\delta_H$ 2.63 and 1.96 ppm). The HMBC spectrum (**Figure 8**) revealed that H-1 correlate to C-3/C-9/C-5, confirming the presence of an olefinic bonded to C-1 and C-2 and a carbonyl group at C-3. The presence of a hydroxyl group was supported by HMBC correlations between H-30 and C-7/H-7 and C-9, indicating Carbon 7 has an attached hydroxyl group. The positions of the carbonyl and epoxide groups were identified through correlations between H17 and C-12,13, and correlations between H-17 and H-15 with C-16 ($\delta_C$ 209.5 ppm). Further correlations between H-17/C-20, C-21 and C-22. At carbon 17, a furan ring was detected.

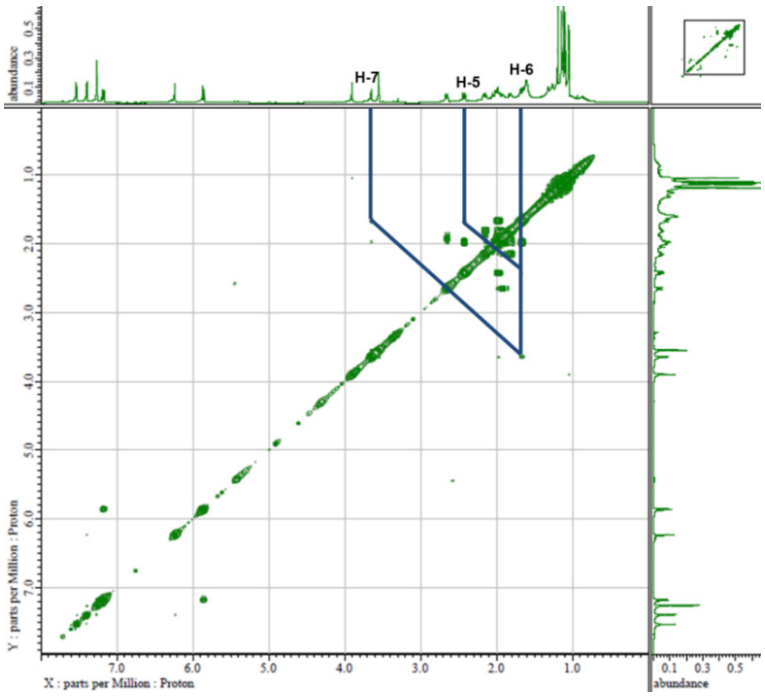


**Figure 7** $^{1}$H-$^{1}$H COSY spectrum of (**1**).

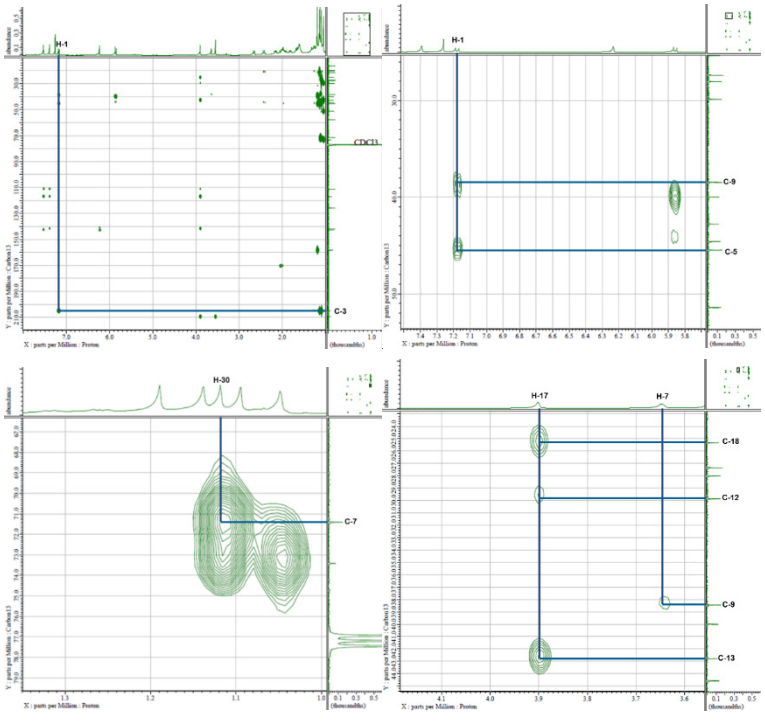


**Figure 8** HMBC spectrum of (**1**).

The relative configuration of the epoxide among C-14/C-15 and the OH bounded to C-7 was set using the NOESY spectrum (**Figure 9**). There were correlations between the sp$^3$-oxygenated methine H-7 and $CH_3$-30 and $CH_3$-19, which are biosynthetically oriented beta, indicating that H-7 was b-oriented and the hydroxyl group attached to C-7 was presumed to be a-oriented. Additionally, there was a correlation between the oxygenated-methine proton sp$^3$ H-15/$CH_3$-18 ($\delta_H$ 1.03), which are biosynthetically a-oriented, suggesting that

H-15 was a-oriented and the epoxide between C-14/C-15 was b-oriented. The spectral correlations for compound **1** were illustrated in **Figure 10**. Compound **1** was elucidated as the known compound 7-deacetylepoxyazadInfraredadione (**1**) [25].

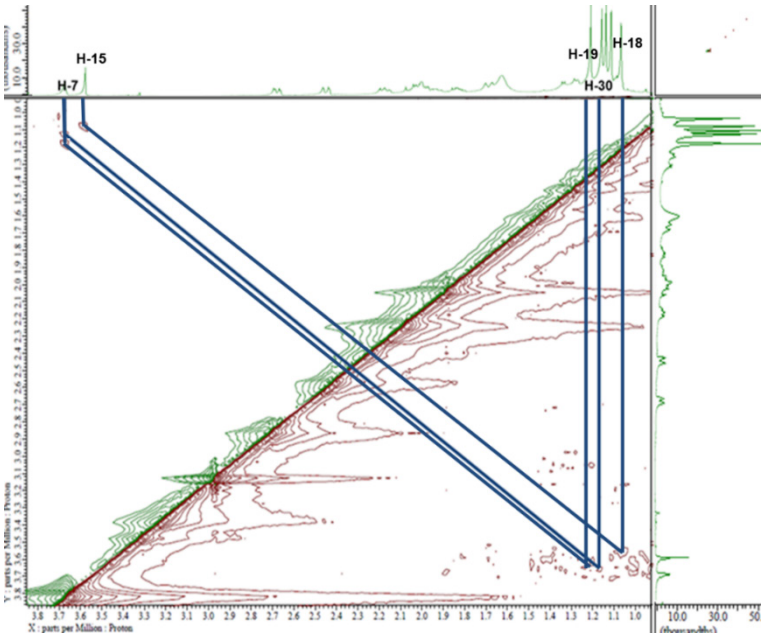


**Figure 9** NOESY spectrum of (**1**).

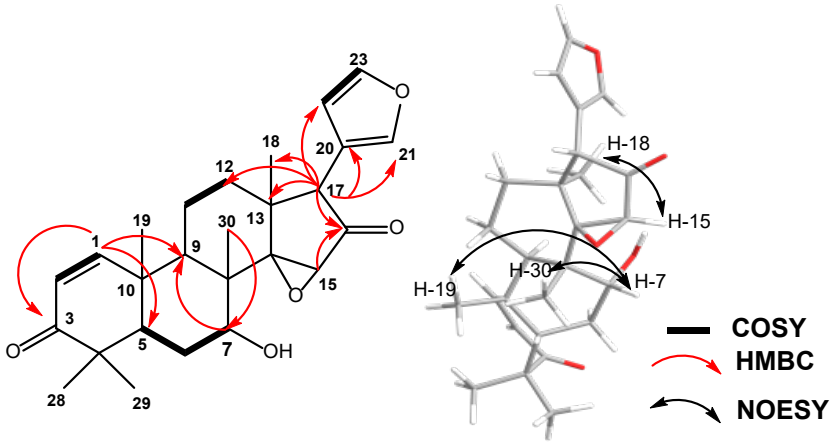


**Figure 10** The HMBC, $^{1}$H-$^{1}$H-COSY and NOESY correlations of compound **1**.

A white powder of compound **2** was gained and soluble in acetone and chloroform. Thin-layer chromatography analysis showed a red color after being sprayed with Ehrlich's reagent. Compound **2** fluoresced at l 254 nm but did not appear at l,365 nm. Based on UV spectrum analysis, **2** showed absorption at a wavelength of 215 nm (**Figure 11**). The UV analysis was strengthened with the FTIR spectrum (**Figure 12**), which evidenced absorption at 1,668 $cm^{-1}$ characteristic of unsaturated carbonyl stretching, followed by absorption at 2,922 $cm^{-1}$ (carbon-hydrogen $sp^3$), 1,741 $cm^{-1}$ (carbonyl group), 1,503 $cm^{-1}$ (carbon-carbon double bonds), 1,365 $cm^{-1}$ (*gem*-dimethyl) and 1,244 $cm^{-1}$ (carbon-oxygen stretching). Compound **2** differed from compound **1** in that it did not have a hydroxyl group.

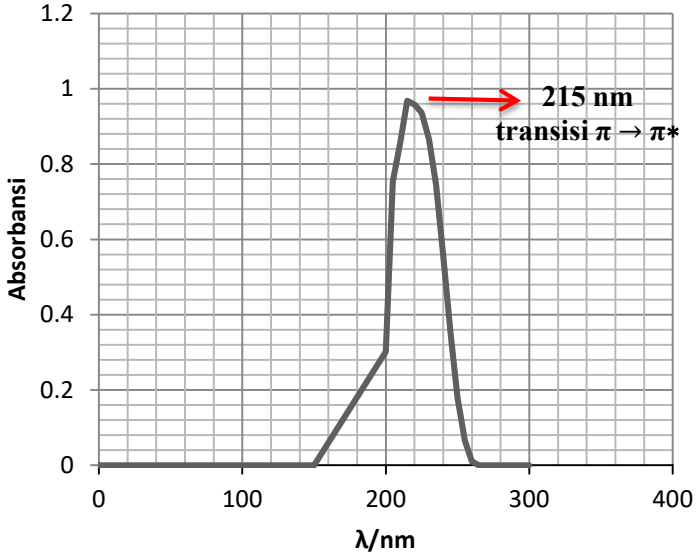


**Figure 11** UV spectrum of (**2**).

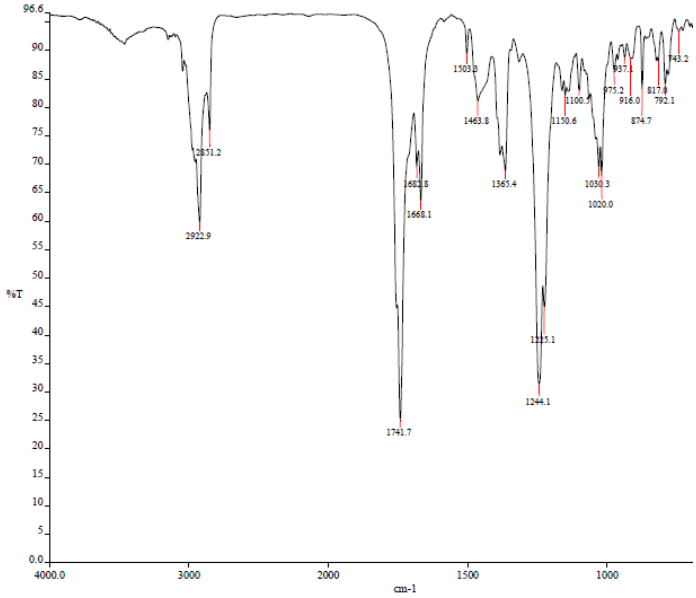


**Figure 12** FT-IR spectrum of (**2**).

The appearance of ion molecular peak of *m/z* 525.2484 $[M + H]^+$ using HRTOFMS (**Figure 13**) was used to determine the structural formula The calculation for $C_{30}H_{36}O_8$ was *m/z* 525.2488. Therefore, compound **2** had a molecular formula of $C_{30}H_{36}O_8$ with a relative molecular mass of 524.2484 and 13 ° of unsaturation were validated by NMR data. The existence of 5 singlet peaks for tertiary methyl protons and the occurrence of acetyl as a substituent in compound 2 were indicated of proton NMR spectrum (**Figure 14**). with methyl signals (each 3H, singlet) at $\delta_H$ 2.09 and 2.33 ppm. Three oxygenated protons ($sp^3$) were observed at $\delta_H$ 4.54, 5.30 and 5.60. The characteristic signals of furan was also appeared along with 3 olefinic protons at $\delta_H$ [5.85 (1H, d, $J$ = 10.5 Hz), 5.70 (1H, s) and 7.08 (1H, d, $J$ = 10.5 Hz)]. Two characteristic $sp^2$ proton signals at $\delta_H$ 5.85 and 7.08 ppm had the same $J$ value of 10.5 Hz, indicating that these protons were coupled and likely adjacent to a carbonyl group, confirming the attendance of an α,β-unsaturated ketone system in the structure of compound **2**.

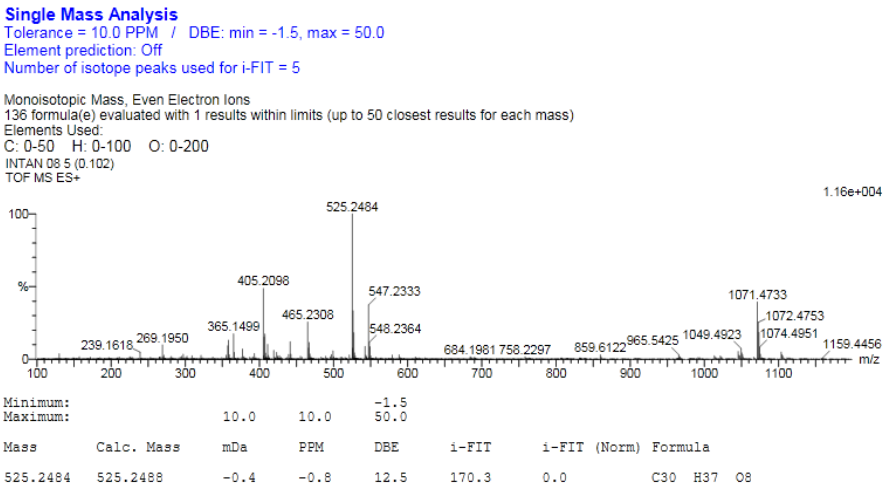


**Figure 13** HRTOF-MS spectrum of (**2**).

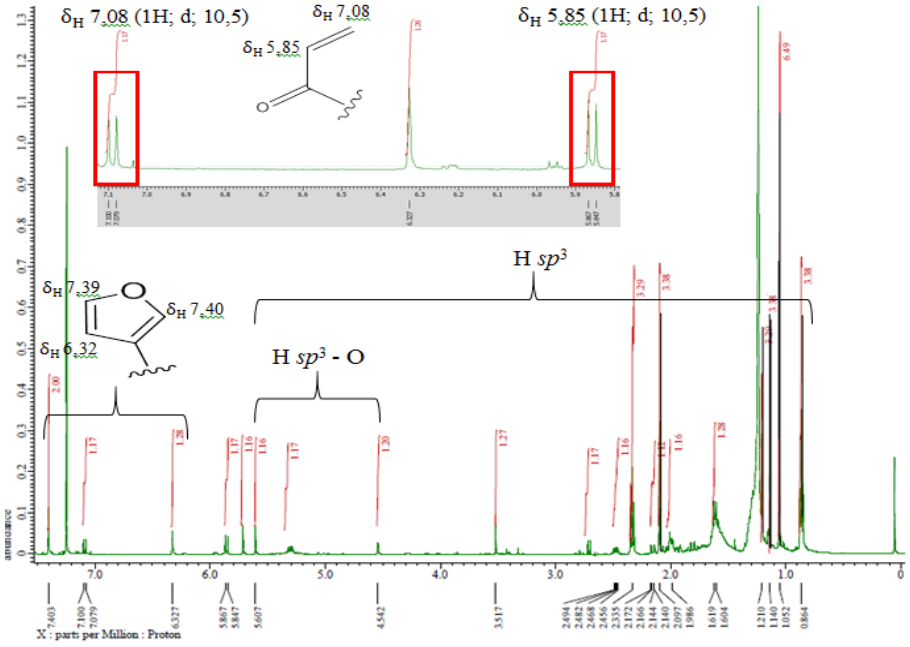


**Figure 14** $^{1}$H-NMR spectra of (**2**) (500 MHz in $CDCl_3$).

The spectrum of $^{13}$C-NMR (**Figure 15**) showed 30 carbon signals, comprising 5 methyl groups at $\delta_C$ 18.4, 19.8, 22.7, 24.7 and 27.2 ppm. Additionally, there were 2 substituents of acetyl at C-1'/C-1"/C-2' and C-2". Two methylene groups appeared at $\delta_C$ 14.2 and 26.0 ppm and 2 $sp^3$ methine groups at $\delta_C$ 40.1 and 46.1 ppm. Four $sp^2$ methine groups were observed at $\delta_C$ 109.9, 111.0, 126.0 and 157.0 ppm, while 3 oxygenated $sp^3$ methine groups appeared at $\delta_C$ 69.8, 73.3, and 78.3 ppm. Two oxygenated $sp^2$ methine groups were found at $\delta_C$ 141.2 and 143.1 ppm. Four $sp^3$ quaternary carbons were at $\delta_C$ 38.8, 39.5, 42.6 and 44.1 ppm, and 2 Cqs ($sp^2$) were at $\delta_C$ 120.4 and 158.2 ppm. Finally, 2 carbonyl groups were present at $\delta_C$ 167.5 and 204.1 ppm. This elucidation was confirmed by HMQC spectrum (**Figure 16**) which unveiled correlations H-19/ C-19, H-30/C-30, H-28/ C-28, H-29/C-29 and H-18/C-18, proving the presence of 5 tertiary methyl groups ($\delta_C$ 18.4, 22.7, 27.2, 19.8 and 24.7 ppm). The correlations of H-1"/C-1" and H-1'/C-1' ($\delta_C$ 21.1 and 21.2 ppm) confirmed 2 acetyl groups on compound **2**. Correlations of H-7/C-7, H-6/C-6 and H-17/C-17 indicated 3 oxygenated $sp^3$ methine groups, suggesting 2 acetyl and 1 additional ester group. Correlations of H-1/C-1, H-2/C-2, H-15/C-15 and H-

22/C-22 confirmed 4 $sp^2$ methine groups, and the signal showed H-21/C-21 and H-23/C-23 ($\delta_C$ 143.1 ppm) substantiated 2 oxygenated $sp^2$ methine groups, reinforcing the existence of a furan ring.

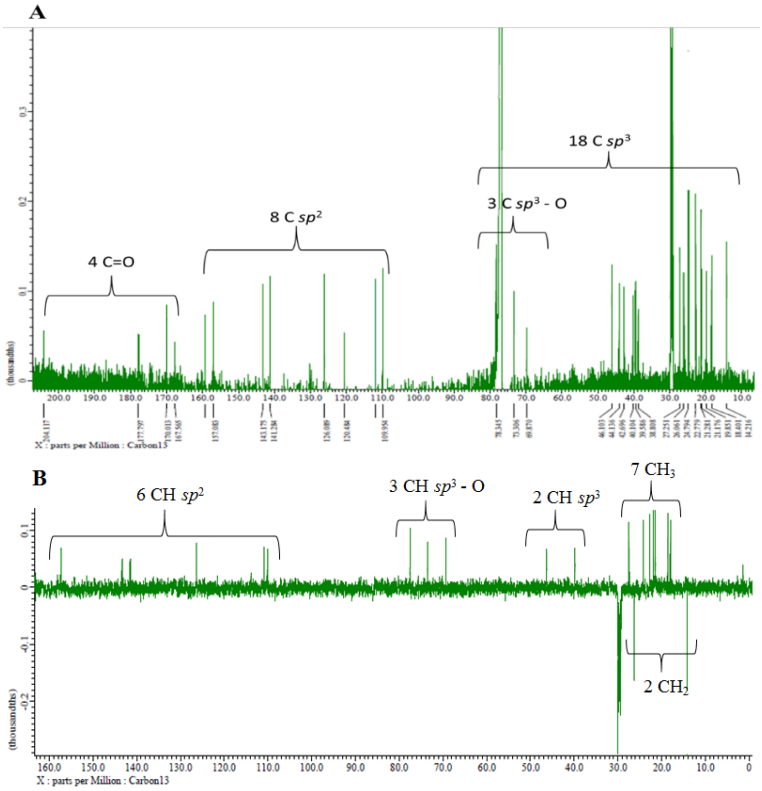


**Figure 15** $^{13}$C-NMR (A) and DEPT 135 (B) spectra of (**2**) (125 MHz in $CDCl_3$).

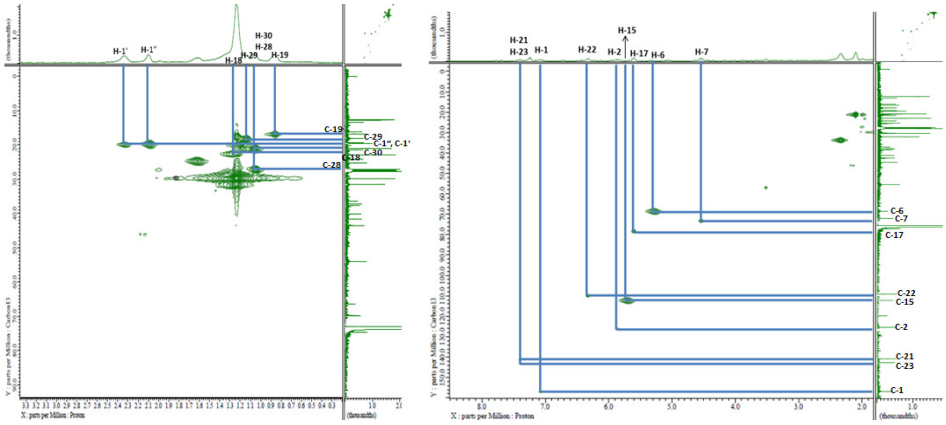


**Figure 16** Spectrum HMQC of (**2**).

The $^1$H-$^1$H COSY spectrum (**Figure 17**) displayed correlations between H-1/H-2 ($\delta_H$ 7.08/5.85 ppm), H-22 and H-23 ($\delta_H$ 6.32 and 7.39 ppm), H-6-H-5/H-7 ($\delta_H$ 5.30 with 2.70 and 4.54 ppm) and H-11-H-9/H-12 ($\delta_H$ 1.61 with 2.47 and 1.98 ppm).

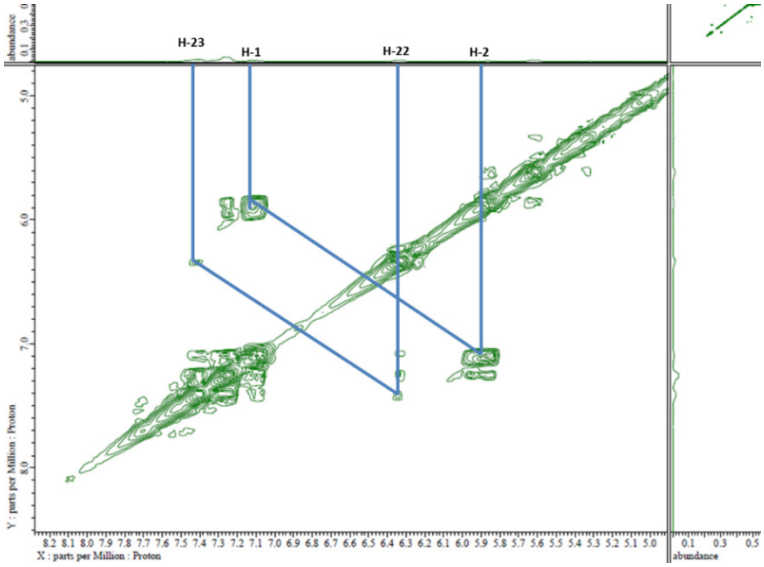


**Figure 17** $^{1}$H-$^{1}$H COSY spectrum of (**2**).

The HMBC spectrum (**Figure 18**) revealed correlations between H-1/C-3/C-5 and H-2/C-10, confirming the presence of an olefinic bond between C-1 and C-2 and a C=O at C-3. Two acetyl groups on compound **2** were confirmed by HMBC correlations between H-6/C-8 and H-7/C-9. Further correlations of H-6/C-2', H-7/C-2", H-1'/C-2' and H-1" ($\delta_H$ 2.09 ppm) with C-2" ($\delta_C$ 170.0 ppm) indicated that the groups composed of acetyl were added to C-6 and C-7. The ester carbonyl group, previously identified by its chemical shift at $\delta_C$ 167.5 ppm, was positioned through HMBC connections among H-17/C-16 ($\delta_H$ 5.60/167.5 ppm) and C-13 ($\delta_C$ 38.8 ppm) and between H-15 ($\delta_H$ 5.70 ppm) with C-16 ($\delta_C$ 167.5 ppm) and C-14 ($\delta_C$ 158.2 ppm), confirming the ester carbonyl at C-16 and a double bond between C-14 and C-15 ($\delta_C$ 158.2 and 111.0 ppm). Additionally, correlations between H-17 ($\delta_H$ 5.60 ppm) with C-20 ($\delta_C$ 120.4 ppm), C-21 ($\delta_C$ 141.2 ppm) and C-22 ($\delta_C$ 109.9 ppm) confirmed that the furan ring was attached at C-17.

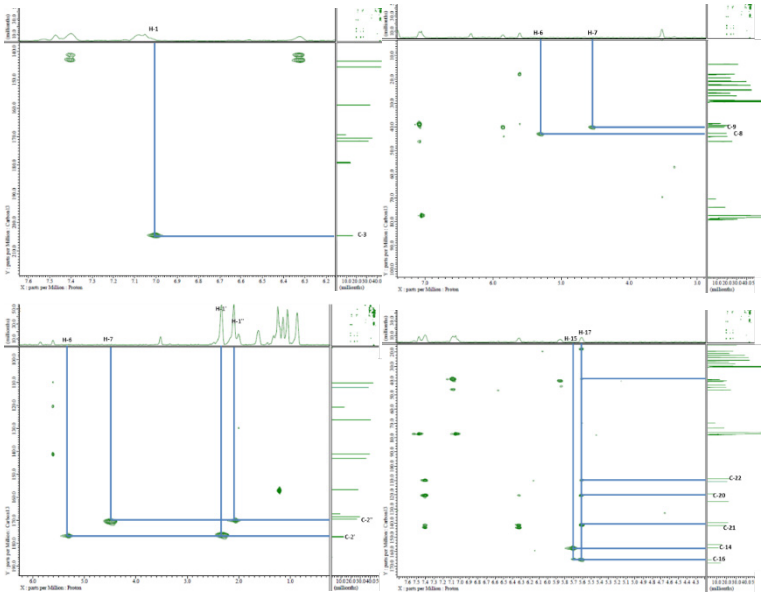

**Figure 18** HMBC spectrum of (**2**).

Based on analysis of all data spectra, the structural type of compound **2** was different with **1** but similar to compound **3**. Compound **2** was reported for the first time in this genus. $^{1}$H-$^{1}$H COSY and HMBC correlations for compound **2** were illustrated in **Figure 19**.

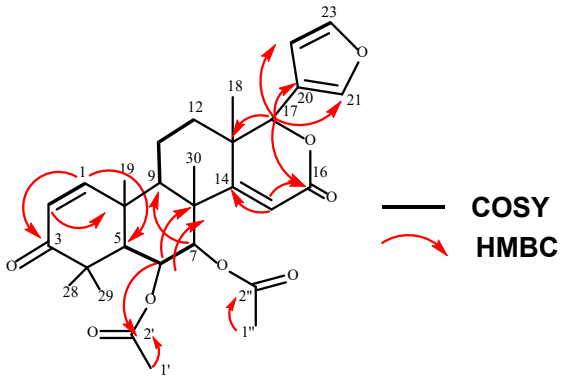


**Figure 19** The HMBC and $^{1}$H-$^{1}$H-COSY correlations of compound **2**.

Compound **2** exhibited a different cyclic structure compared to compound **1**. A thorough review of the NMR spectrum information and contrast with previously published findings confirmed compound **2** as 6α-acetoxydeoxygedunin, similar to compound **3** [27]. This suggestion was based on the analysis of UV, IR and NMR spectra (**Figures 20 - 23**) of compound **3**, and was supported by the addition of 1 oxygen atom, resulting in a molecular ion signal in the HRTOFMS spectrum with *m/z* 541.2440 $[M + H]^{+}$ (**Figure 24**). The chemical shift in compound **3** supported this proposal. The primary difference lay in the chemical shifts at C-14-C-15. In compound **3**, these shifts corresponded to $sp^{3}$-oxidized carbons, while in compound **2**, the shifts indicated $sp^{2}$ carbons with C-14 and C-15. Thus, compound **3** has been recognized as 6α-acetoxygedunin.

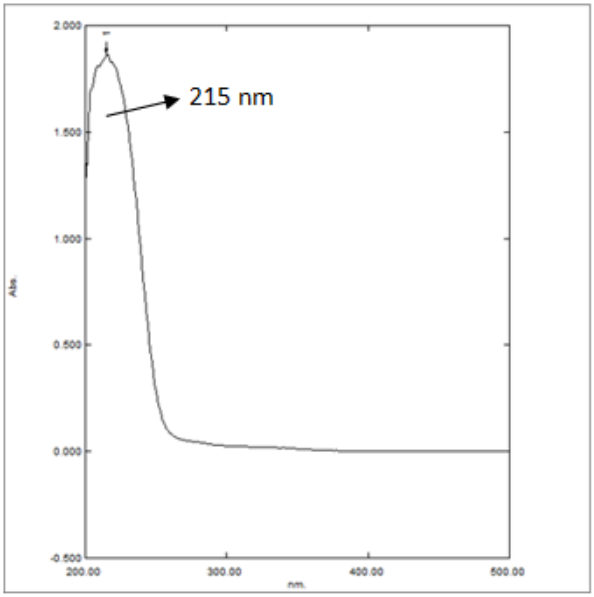


**Figure 20** UV spectrum of (**3**).

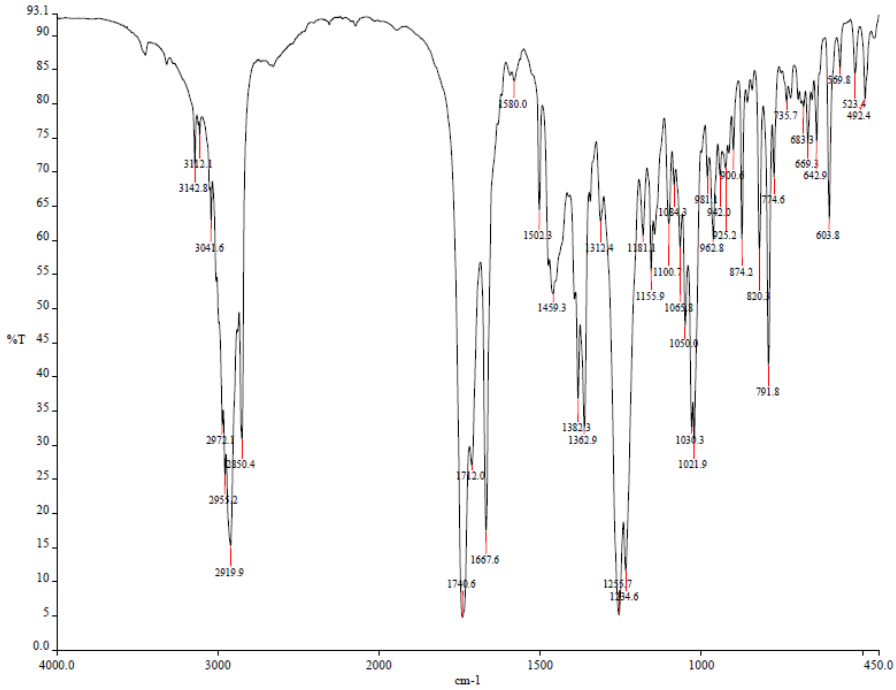


**Figure 21** FT-IR spectrum of (**3**).

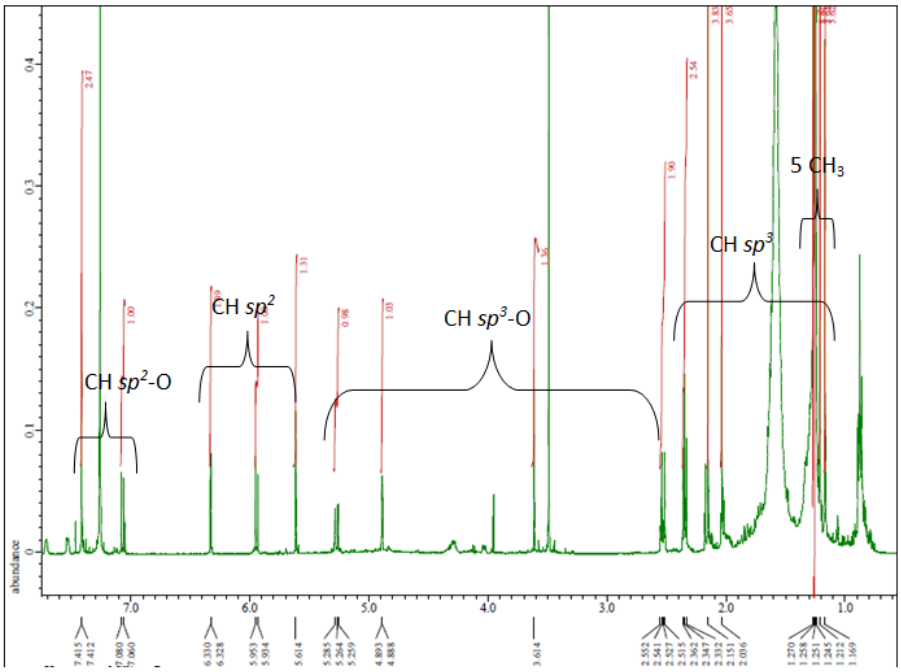


**Figure 22** $^1$H-NMR spectra of (**3**) (500 MHz in $CDCl_3$).

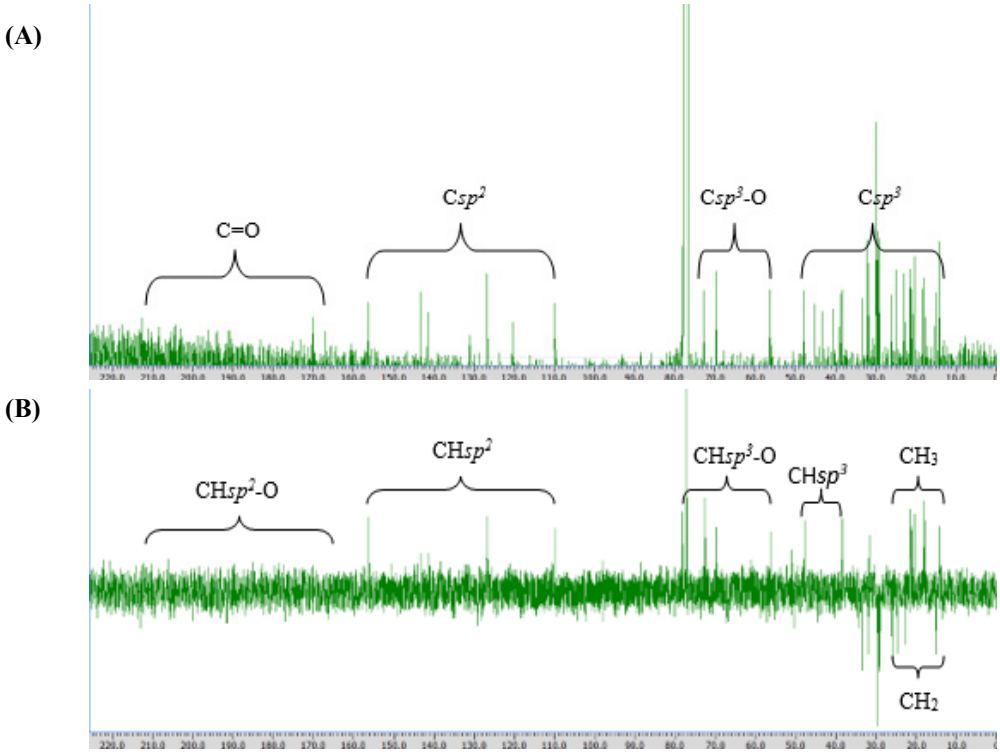


**Figure 23** $^{13}$C-NMR (A) and DEPT 135 (B) spectra of (**3**) (125 MHz in $CDCl_3$).

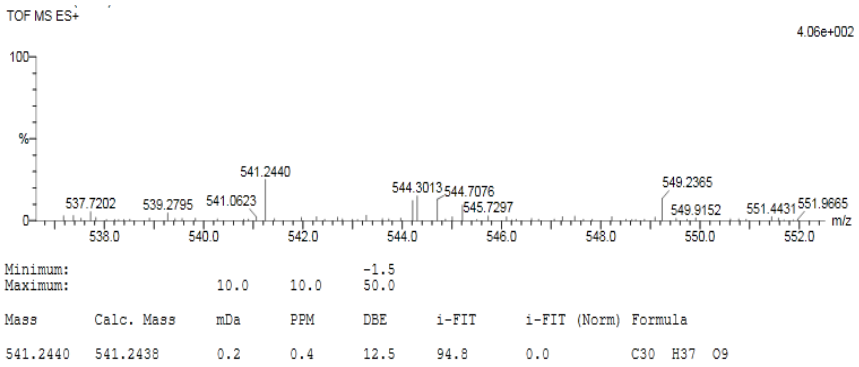


| | | | | | | | |
|---|---|---|---|---|---|---|---|
| Minimum: | | | | -1.5 | | | |
| Maximum: | | 10.0 | 10.0 | 50.0 | | | |
| Mass | Calc. Mass | mDa | PPM | DBE | i-FIT | i-FIT (Norm) | Formula |
| 541.2440 | 541.2438 | 0.2 | 0.4 | 12.5 | 94.8 | 0.0 | C30 H37 O9 |

**Figure 24** HRTOF-MS spectrum of (**3**).

The comparison of compounds **1**, **2** and **3** is shown in **Figure 25**. Compound **1** had a havanensin-type limonoid skeleton, while compounds **2** and **3** had a gedunin-type limonoid skeleton with a lactone on the D ring. Based on previous structural elucidation, the differences among compounds **1**, **2** and **3** lay only in the substituents attached to the limonoid skeletons. For example, the substituents attached to carbon numbers 6 and 7 of the limonoid skeleton. In compounds 2 and 3, there were acetyl groups attached to carbons 6 and 7, indicated by 2 proton shifts around 2 ppm for the acetyl methyl protons and 2 carbon shifts around 170 ppm for the acetyl carbonyl. In contrast, compound 1 did not have acetyl substituents on carbons 6 and 7, instead, it had a hydroxyl group attached to carbon 7. This was marked by a carbon shift for the $sp^3$-oxidized methine and a characteristic OH stretch absorption in the infrared spectrum.

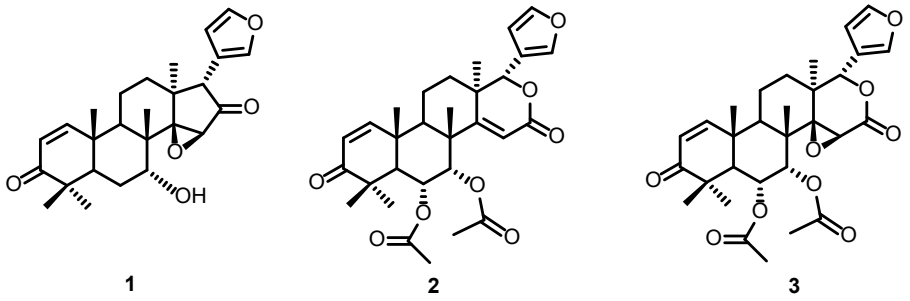

**Figure 25** Chemical structures of limonoids **1 - 3**.

**The cytotoxicity of compounds (1 - 3)**

The cytotoxic properties of limonoids **1** - **3** have been studied on the MCF-7 cancer cells. Cisplatin with $IC_{50}$ of 38.06 µg/mL, acted as the positive control. The findings were provided in **Table 1** and **Figure 26**. Among all limonoids, 6α-acetoxydeoxygedunin (**2**) exhibited the greatest cytotoxic activity, whereas 7-deacetylepoxyazadInfraredadione (**1**) demonstrated the weakest activity. Based on data from the Widiyastuti *et al.* [28], cytotoxic compounds are categorized into 4 categories: Highly harmful ($IC_{50} \leq 20$ µg/mL), fairly cytotoxic ($IC_{50}$ 21 - 200 µg/mL), mildly cytotoxic ($IC_{50}$ 201 - 500 µg/mL) and non-toxic ($IC_{50} > 500$ µg/mL). Based on these benchmarks, compound **1** was classified as non-cytotoxic, with an $IC_{50}$ value exceeding 500 µg/mL. In contrast, compounds **2** and **3** were categorized as weakly cytotoxic, with $IC_{50}$ values of 231.26 and 475.87 µg/mL, respectively. Although their activity was weaker than that of cisplatin, these findings remain therapeutically relevant, as weak cytotoxicity does not rule out the potential for further optimization or synergistic effects when combined with other agents. The difference in activity between compounds **2** and **3** likely results from variations in their molecular structures. Specifically, 6α-acetoxydeoxygedunin (**2**) contains a double bond between C-14 and C-15, while 6α-acetoxygedunin (**3**) has an epoxide group at the same position. The higher cytotoxicity of compound 2 suggested that the presence of an epoxide at C-14/C-15 in compound **3** may reduce cytotoxic activity.

Moreover, the ongoing demand for new anticancer agents encourages the investigation of compounds with diverse activities beyond immediate potency. Even compounds that do not exhibit high cytotoxicity could be optimized for specific cancer cell lines or other therapeutic targets, including anti-inflammatory or chemo preventive properties [29]. These insights highlight the importance of continuing research into limonoids despite their initially weak cytotoxicity, as they hold potential for future drug development through targeted improvements and combination strategies.

**Table 1** Cytotoxicity activity of compounds **1** - **3** against MCF-7 cancer lines.

| Limonoid compounds | $IC_{50}$ (µg/mL) |
|---|---|
| 7-deacetylepoxyazadInfraredadione (**1**) | > 500 |
| 6α-acetoxydeoxygedunin (**2**) | 231.26 |
| 6α-acetoxygedunin (**3**) | 475.87 |
| Cisplatin (+) | 38.06 |

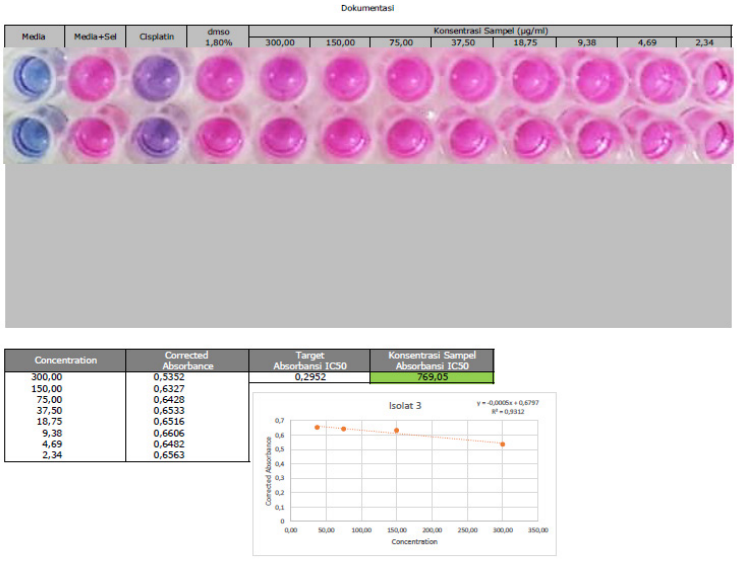


| Concentration | Corrected Absorbance |
|---|---|
| 300,00 | 0,5352 |
| 150,00 | 0,6327 |
| 75,00 | 0,6428 |
| 37,50 | 0,6533 |
| 18,75 | 0,6516 |
| 9,38 | 0,6606 |
| 4,69 | 0,6482 |
| 2,34 | 0,6563 |

| Target Absorbansi IC50 | Konsentrasi Sampel Absorbansi IC50 |
|---|---|
| 0,2952 | 769,05 |




**(A)**

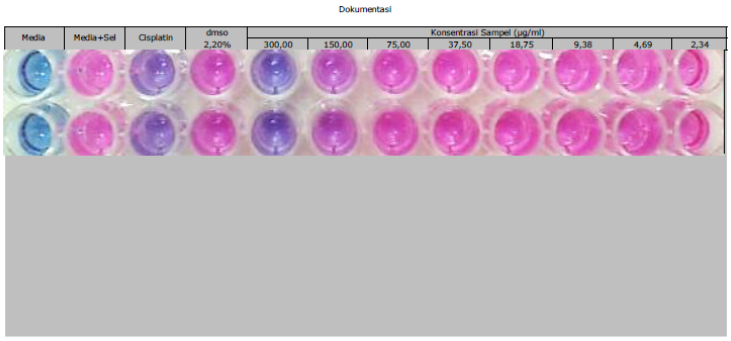


| Concentration | Corrected Absorbance |
|---|---|
| 300,00 | 0,1833 |
| 150,00 | 0,4462 |
| 75,00 | 0,6409 |
| 37,50 | 0,6679 |
| 18,75 | 0,6837 |
| 9,38 | 0,6835 |
| 4,69 | 0,6881 |
| 2,34 | 0,6807 |

| Target Absorbansi IC50 | Konsentrasi Sampel Absorbansi IC50 |
|---|---|
| 0,3005 | 231,26 |

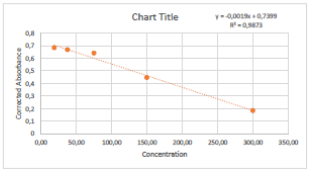


**(B)**

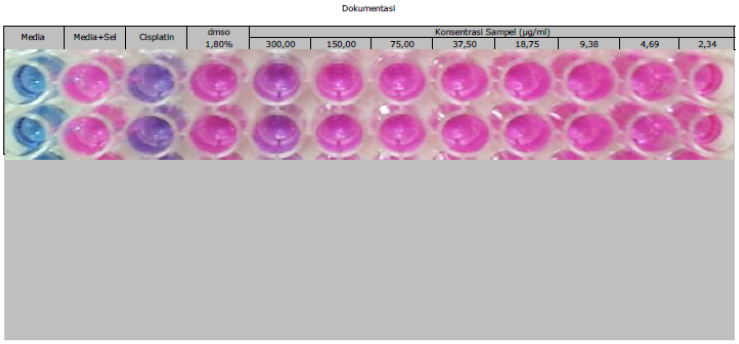


| Concentration | Corrected Absorbance |
|---|---|
| 300,00 | 0,4337 |
| 150,00 | 0,6112 |
| 75,00 | 0,6427 |
| 37,50 | 0,6409 |
| 18,75 | 0,6639 |
| 9,38 | 0,6794 |
| 4,69 | 0,6751 |
| 2,34 | 0,6712 |

| Target Absorbansi IC50 | Konsentrasi Sampel Absorbansi IC50 |
|---|---|
| 0,3061 | 475,87 |

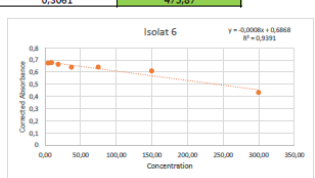


**(C)**

**Figure 26** The statistical analysis of cytotoxicity results; compound 1 (A), compound 2 (B) and compound 3 (C).

## Conclusions

The 7-deacetylepoxyazadInfraredadione (**1**), 6α-acetoxydeoxygedunin (**2**) and 6α-acetoxygedunin (**3**) were 3 limonoid compounds, which were successfully isolated and identified from *Chisocheton macrophyllus* seeds. The bioactivity of these 3 compounds has been tested to cancer cells (MCF-7 cells). Among them, 6α-acetoxydeoxygedunin (**2**) denoted the greatest cytotoxic activity, while 7-deacetylepoxyazadInfraredadione (**1**) showed the least activity. This difference in cytotoxicity can be seen based on SAR, where the C14 and C15 positions of compound **2** have a conjugated double bond, which has the effect of increasing the activity of **2** compared to compound **3**, which has an epoxide at this position. These findings underline the potential of limonoid compounds, especially compound **2**, as promising candidates for further development as anticancer agents, highlighting their structural features that are important for bioactivity in cancer treatment research and can be developed as target molecules through study able mechanisms for the discovery of new drugs.

## References

[1] GM Happi and R Teufel. Steroids from the Meliaceae family and their biological activities. *Phytochemistry* 2024; **221**, 114039.

[2] AT Hidayat, K Farabi, D Harneti, R Maharani, N Darwati, T Mayanti and Y Shiono. Cytotoxicity and structure-activity relationship of Dammarane-type triterpenoids from the bark of *Aglaia elliptica* against P-388 murine leukemia cells. *Natural Product Sciences* 2017; **23(4)**, 291-298.

[3] MA Ngadni, SL Chong, H Hazni, N Asib, IH Ishak, NM Misnan and K Awang. Limonoids from the fruits of *Chisocheton erythrocarpus* and their mosquito larvicidal activities. *Phytochemistry* 2024; **222**, 114092.

[4] U Supratman, W Naibaho, S Salam, R Maharani, AT Hidayat, D Harneti and Y Shiono. Cytotoxic triterpenoids from the bark of *Chisocheton patens* Blume (Meliaceae). *Phytochemistry Letters* 2019; **30**, 81-87.

[5] T Mayanti, SE Sinaga and U Supratman. Phytochemistry and biological activity of *Lansium domesticum* Corr. species: A review. *Journal of Pharmacy and Pharmacology* 2022; **74(11)**, 1568-1587.

[6] F Mulani, S Nandikol and H Thulasiram. Chemistry and biology of novel Meliaceae limonoids. *Biological and Medicinal Chemistry* 2022. http://dx.doi.org/10.26434/chemrxiv-2022-2bpb9-v2

[7] S Fu and B Liu. Recent progress in the synthesis of limonoids and limonoid-like natural products. *Organic Chemistry Frontiers* 2020; **7(14)**, 1903-1947.

[8] P Zhang, S Xue, W Huang, C Wang, Z Cui, J Luo and L Kong. Diverse prieurianin-type limonoids with oxygen-bridged caged skeletons from two *Aphanamixis* species: Discovery and biomimetic conversion. *Organic Chemistry Frontiers* 2021: **8(3)**, 566-571.

[9] MJ Durán-Peña, JM Botubol-Ares, IG Collado and R Hernandez-Galán. Degraded limonoids: Biologically active limonoid fragments re-enhancing interest in Meliaceae and Rutaceae sources. *Phytochemistry Reviews* 2023; **22(3)**, 695-741.

[10] TM Braga, L Rocha, TY Chung, RF Oliveira, C Pinho, AI Oliveira and A Cruz. Biological activities of gedunin - A limonoid from the Meliaceae family. *Molecules* 2020; **25(3)**, 493.

[11] W Fan, L Fan, Z Wang and L Yang. Limonoids from the genus *Melia* (Meliaceae): Phytochemistry, synthesis, bioactivities, pharmacokinetics, and toxicology. *Frontiers in Pharmacology* 2022; **12**, 795565.

[12] TN Tan, HT Trung, Q Le Dang, HV Thi, HD Vu, TN Ngoc, HT Thi Do, TH Nguyen, DN Quang and TT Dinh. Characterization and antifungal activity of limonoid constituents isolated from Meliaceae plants *Melia dubia*, *Aphanamixis polystachya*, and *Swietenia macrophylla* against plant pathogenic fungi *in vitro*. *Journal of Chemistry* 2021; **2021**, 4153790.

[13] JA Shilpi, S Saha, SL Chong, L Nahar, SD Sarker and K Awang. Advances in chemistry and bioactivity of the genus *Chisocheton* Blume. *Chemistry & Biodiversity* 2016; **13(5)**, 483-503.

[14] Supriatno, Nurlelasari, T Herlina, D Harneti, R Maharani, AT Hidayat and Y Shiono. A new

limonoid from stem bark of *Chisocheton pentandrus* (Meliaceae). *Natural Product Research* 2018; **32(21)**, 2610-2616.

[15] K Mohamad, Y Hirasawa, CS Lim, K Awang, AHA Hadi, K Takeya and H Morita. Ceramicine A and walsogyne A, novel limonoids from two species of Meliaceae. *Tetrahedron Letters* 2008; **49(27)**, 4276-4278.

[16] W Maneerat, S Laphookhieo, S Koysomboon and K Chantrapromma. Antimalarial, antimycobacterial and cytotoxic limonoids from *Chisocheton siamensis*. *Phytomedicine* 2008; **15(12)**, 1130-1134.

[17] K Awang, CS Lim, K Mohamad, H Morita, Y Hirasawa, K Takeya, O Thoison and AHA Hadi. Erythrocarpines A-E, new cytotoxic limonoids from *Chisocheton erythrocarpus*. *Bioorganic & Medicinal Chemistry* 2007; **15(17)**, 5997-6002.

[18] MH Yang, JS Wang, JG Luo, XB Wang and LY Kong. Tetranortriterpenoids from *Chisocheton paniculatus*. *Journal of Natural Products* 2009; **72(11)**, 2014-2018.

[19] IA Najmuldeen, AHA Hadi, K Awang, K Mohamad and SW Ng. 14-Deoxyxyloccensin K from *Chisocheton ceramicus* (Meliaceae). *Acta Crystallographica Section E: Structure Reports Online* 2010; **66(8)**, o1927-o1927.

[20] Nurlelasari, I Rahmayanti, S Salam, A Safari, D Harneti, R Maharani and U Supratman. A new havanensin-type limonoid from *Chisocheton macrophyllus*. *Applied Biological Chemistry* 2021; **64**, 35.

[21] KC Murthy, GK Jayaprakasha, S Safe and BS Patil. Citrus limonoids induce apoptosis and inhibit the proliferation of pancreatic cancer cells. *Food & Function* 2021; **12(3)**, 1111-1120.

[22] S Shaheen, S Khalid, K Aaliya, A Gul, A Hafeez, M Armaghan and J Sharifi-Rad. Insights into Nimbolide molecular crosstalk and its anticancer properties. *Medical Oncology* 2024; **41(6)**, 158.

[23] F Bray, M Laversanne, H Sung, J Ferlay, RL Siegel, I Soerjomataram and A Jemal. Global cancer statistics 2022: GLOBOCAN estimates of incidence and mortality worldwide for 36 cancers in 185 countries. *CA: A Cancer Journal for Elinicians* 2024; **74(3)**, 229-263.

[24] SE Sinaga, M Fajar, T Mayanti and U Supratman. Bioactivities screening and elucidation of terpenoid from the stem bark extracts of *Lansium domesticum* Corr. cv. *Kokosan* (Meliaceae). *Sustainability* 2023; **15(3)**, 2140.

[25] PA Yadav, CP Kumar, B Siva, KS Babu, AD Allanki, PS Sijwali and AV Rao. Synthesis and evaluation of anti-plasmodial and cytotoxic activities of epoxyazadiradione derivatives. *European Journal of Medicinal Chemistry* 2017; **134**, 242-257.

[26] T Suzuki, NR Ariefta, T Koseki, H Furuno, E Kwon, H Momma, D Harneti, R Maharani, U Supratman, K Kimura and Y Shiono. New polyketides, paralactonic acids A - E produced by *Paraconiothyrium* sp. SW-B-1, an endophytic fungus associated with a seaweed, *Chondrus ocellatus* Holmes. *Fitoterapia* 2019; **132**, 75-81.

[27] Y Tanaka, T Yamada, Y In, O Muraoka, T Kajimoto and R Tanaka. Absolute stereostructure of Andirolides A - G from the flower of *Carapa guianensis* (Meliaceae). *Tetrahedron* 2011; **67(4)**, 782-792.

[28] Y Widiyastuti, IYM Sholikhah and S Haryanti. Cytotoxic activities of ethanolic and dichloromethane extract of leaves, stems, and flowers of Jarong [*Stachytarpheta jamaicensis* (L.) Vahl.] on HeLa and T47D cancer cell line. *AIP Conference Proceedings* 2019; **2202**, 020101.

[29] RH Shoemaker. The NCI60 human tumour cell line anticancer drug screen. *Nature Reviews Cancer* 2006; **6(10)**, 813-823.